



Research Article

ISSN : 0975-7384
CODEN(USA) : JCPRC5

Development and characterization of oil shale minerals for ciprofloxacin remediation

Asmae Gouza¹, Sanaâ Saoiabi¹, Sylvie Masse², Abdelaziz Laghzizil^{1*} and Ahmed Saoiabi¹

¹Laboratoire de Chimie Physique Générale, Faculté des Sciences, Université Mohamed V, Rabat, Morocco

²Université Pierre et Marie Curie; CNRS, Chimie de la Matière Condensée de Paris, Collège de France, Paris, France

ABSTRACT

A characterization of the Moroccan oil shale was carried out to determine the mineralogical and chemical characteristics. Thermal analysis, x-ray diffraction and infrared techniques were used to study the thermal and the structure behaviors of the Moroccan oil shale from Tanger (OST). The TG analysis showed that the investigated mineral exhibited about 8% as total mass loss containing up 80wt.% of quartz-SiO₂ with less CaO content (<1%). Batch adsorption experiments were conducted to investigate the removal of ciprofloxacin antibiotic from wastewater by addition of OST shale. The best adsorption was obtained with dried OST and calcined at 550°C, which are promising materials for antibiotic removal.

Keywords: Oil shale, Thermal treatment, Characterization, Adsorption

INTRODUCTION

Serious problem of environmental pollution in recent years is due to the presence of antibiotics in aqueous wastewaters from many sources such as pharmaceutical industry, domestic and hospital wastes, and chemical manufacturing [1-4]. In fact, the water pollution is mainly caused by a strong industrialization which rejects toxic pollutants without any prerequisite treatment [5]. Antibiotics have been used in large quantities for several decades as human and veterinary medicine as well as husbandry growth promoters [6-7]. They were detected in municipal wastewater, surface water and ground water [8-9]. Among them, ciprofloxacin residues are extensively used and found in various aquatic systems [10-11]. For remediation, a significant current trend in natural and low-cost sorbents with well-defined surface characteristics, chemical and thermal stability [12-13]. Among of them, shale is considered as the vastest energy resources in the world, which exists in Morocco with large quantity, the most important fields are in Timahdit, Tarfaya and Tanger [14]. It is evident that OST contains a wide variety of acidic, basic and amphoteric oxides, whose major chemical and mineral compositions are silicon dioxide (SiO₂), alumina (Al₂O₃), iron oxide (Fe₂O₃), calcite [CaCO₃], illite [K(Al,Fe)₂AlSi₃O₁₀(OH)₂H₂O], kaolinite [Al₄(Si₃O₁₀)(OH)₆], chlorite [(Mg,Fe)₅(Al, Si)₅O₁₀(OH)₈] [15]. These chemical and physical properties suggest that OST have good adsorption behavior for both organic and inorganic pollutants found in wastewater [16-22]. For this reason, the intention of this paper is to study the adsorptive capabilities and kinetics of Moroccan oil shale as a possible adsorbent to reduce the selected ciprofloxacin antibiotic concentration in water.

EXPERIMENTAL SECTION

2.1 Adsorbent materials and reagents

The naturally oil shale was collected from Tanger-Morocco, which was crushed and grounded to 100-200 µm. The OST was mixed with warm water and stirred for 30 min in order to dissolve the soluble portion. Finally, the resulting mixture was separated by filtration, and washed with distilled water and then dried at 100 °C in air for 24 h

(noted OST100). Finally, OST100 was heat treated at 550°C (noted OST550) and at 950°C (noted OST950) in air for 3 hours. The amounts of chemical constituents in oil shale (OST100) from Tanger are as follows: 80% SiO₂, 7.9% Al₂O₃, 2.17% Fe₂O₃, 1.21% MgO, 0.84% CaO, 0.64% K₂O, 0.31% Na₂O, 0.2% TiO₂, 0.14% ZnO, 0.1% SO₃. We notice that the percentage of SiO₂ is very important, while that of CaO is very low. Ciprofloxacin (1-cyclopropyl-6-fluoro-4-oxo-7-piperazin-1-yl-quinoline-3-carboxylic acid, CIP) was purchased from LNCM Rabat (Morocco).

2.2. Techniques

The resulting solids were characterized using x-ray powder diffraction (Philips PW131 diffractometer). Infrared spectra were recorded at a 2 cm⁻¹ resolution from 400 to 4000 cm⁻¹ on a Brüker IFS 66v Fourier transform spectrometer using KBr pellets. Thermogravimetric and differential thermal analyses were carried out simultaneously in airflow using a TA Instruments Netzsch STA-409EP apparatus. The temperature range is taken from 30 to 1000°C at two heating rates (5°C min⁻¹ and 10°C min⁻¹). Nitrogen adsorption isotherms were recorded at 77 K using a Micromeritics ASAP 2010 instrument. The specific surface area was calculated according to the Brunauer–Emmett–Teller (BET) method using adsorption data in the relative pressure range from 0.05 to 0.25, whereas the pore size and volume were estimated using the Barret–Joyner–Halenda (BJH) approximation.

2.3. Adsorption procedure

Ciprofloxacin adsorption on OST100, OST550 and OST950 adsorbents was studied in batch experiments conducted at 25°C. 200 mg of OST adsorbent was held in contact with 100 mL of solution containing 20 mg L⁻¹ at pH = 5.6 under stirring (250 rpm). At selected time interval, the suspensions were sampled through direct filtration using 0.45 µm membrane filter. The ciprofloxacin concentration in supernatant was monitored using a UV-visible spectrophotometer working at 273 nm controlled by as high performance liquid chromatography (HPLC). The

amount of sorbed antibiotic was calculated by using: $q_t = \frac{C_0 - C_t}{m} \cdot V$ (Eq.1), where q_t is the amount of adsorbed antibiotic at time t (mg g⁻¹), C_0 and $C(t)$ are the antibiotic concentration in solution at $t = 0$ and $t = t$ (mg L⁻¹), V is the volume (L) of the antibiotic solution and m is the weight (g) of the sorbent. All experiments were carried out in triplicate. The mean values are reported and the error range was inferior to 5 %.

In order to determine the kinetics parameters of the sorption reactions, Lagergren pseudo-first and pseudo-second order models have been applied to experimental data. The Lagergren pseudo-first order equation can be expressed as [23]:

$$\log(q_e - q_t) = \log q_{e,1} - \frac{k_1}{2.303} t \quad (\text{Eq.2}), \text{ where } q_e \text{ and } q_{e,1} \text{ are the experimental and calculated amount of}$$

adsorbed antibiotic at equilibrium (mg g⁻¹) and k_1 the first order kinetic constant (min⁻¹). This model can be applied if $\log(q_e - q_t)$ versus t gives a straight line.

The pseudo-second order model can be expressed as a differential equation [24]: $\frac{t}{q_t} = \frac{1}{k_2 q_{e,2}} + \frac{1}{q_{e,2}} t$ (Eq.3),

where $q_{e,2}$ is the calculated amount of adsorbed antibiotic at equilibrium (mg g⁻¹) and k_2 the second order kinetic constant (g mg⁻¹ min⁻¹). The plot of t/q_t against time t of Eq. (3) should give a linear relationship.

Sorption isotherms were analyzed using the Langmuir and Freundlich models. The Langmuir equation can be written as: $\frac{C_e}{q_e} = \frac{1}{\beta q_{e,\max}} + \frac{C_e}{q_{e,\max}}$ (Eq.4), where $q_{e,\max}$ is the calculated maximum amount of adsorbed antibiotic at equilibrium (mg g⁻¹), and β is the Langmuir constant (L.mg⁻¹) related to the adsorption energy. $q_{e,\max}$ and β can be obtained by plotting C_e/q_e vs. C_e .

The Freundlich model can be written as: $q_e = K_f C_e^{1/n}$ (Eq.5) where K_f and n are Freundlich constants, correlated to the maximum adsorption capacity and adsorption intensity, respectively. A linear form of this model is: $\log q_e = \log K_f + 1/n \log C_e$.

RESULTS AND DISCUSSION

3.1. Structure characterization

The crystallographic structure of oil shale from Tanger- Morocco (OST100) was examined by XRD patterns at different temperatures of the calcination (Fig. 1). The high intensity of XRD peaks indicates that OST powder has a high crystallinity. Therefore, the diffractograms of raw material show a main phase attributed to SiO₂-quartz

associated with minority oxide phases as Fe_2O_3 and Al_2O_3 . We note also that no other phases, such as dolomite, are observed in the OST opposite to other oil shales described in the literature [26]. In heating OST100 sample at the temperature up 550°C (OST550) and 950°C (OST950), some reflections disappeared due to the transformation of hydroxyls OH species to the oxide phases and to decomposition of the organic matter connected to raw OST powder.

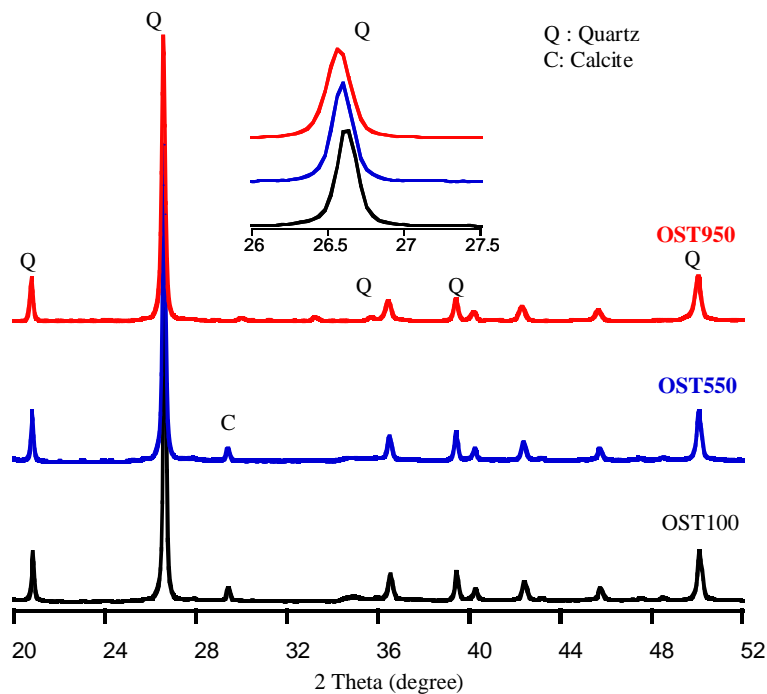


Figure 1. XRD patterns of OST mineral at different temperature of the calcination

Fourier transform infrared spectroscopy shows the main absorption bands at 1170, 1010, 695 and 675 cm^{-1} relative to the SiO_2 groups (Fig.2). Other IR bands towards 1430 and 860 cm^{-1} are attributed to the presence of carbonates, which disappear during the heat treatment especially at 950°C. In the case of the raw OST100, its IR spectrum presents two absorption bands characteristic to the hydroxyl OH ions at 3560 cm^{-1} and 620 cm^{-1} , which are transformed into oxide when the sample is calcined at 950°C. The minority bands due to the presence of carbon chains appeared towards 3380, 2280, 2170, 1969 cm^{-1} .

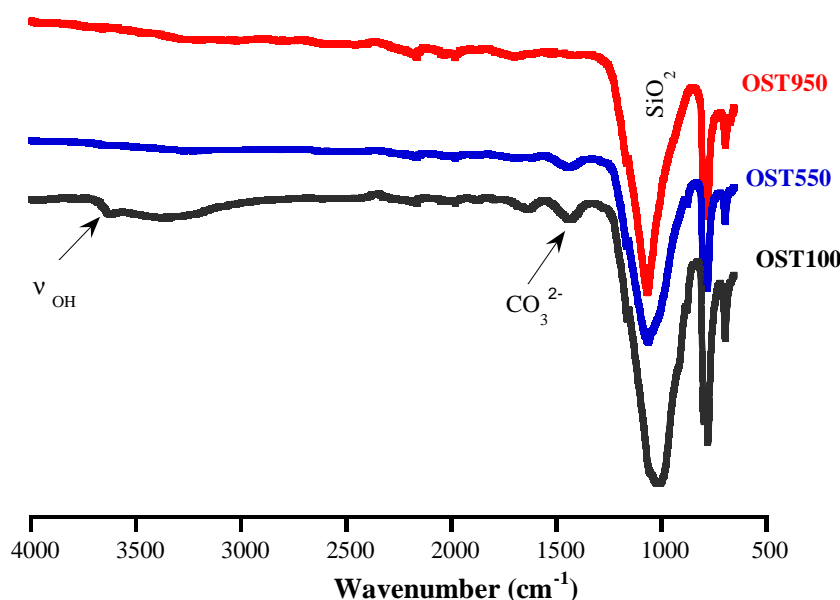


Figure 2. Infrared spectra of OST100, OST550 and OST950 samples

For more information of thermal stability of OST100, TG analysis was realized with two heating rates (5 and $10^{\circ}\text{C min}^{-1}$). Both TG curves show similar profiles with a first step in the $25\text{-}200^{\circ}\text{C}$ temperature range corresponding to weakly-bound water desorption, and a second step between 200°C and 550°C corresponding to the decomposition of some aromatic or nitrogenous organic molecules, whereas the last one is situated between $550\text{-}1000^{\circ}\text{C}$, corresponding to the decomposition of other organic matter with aliphatic carbon chains. The total weight loss at $10^{\circ}\text{C min}^{-1}$ (8.0 %) is slightly superior to that of $5^{\circ}\text{C min}^{-1}$ (7.2%). This small difference is due to the shorter exposure time to a particular temperature at a faster heating rate. We should be noted that although the decomposition temperatures are changed with heating rate, the mass losses remained nearly same. Consequently, the total weight loss is about 8 %, a value lower than those described for other Moroccan oil shale [25-27].

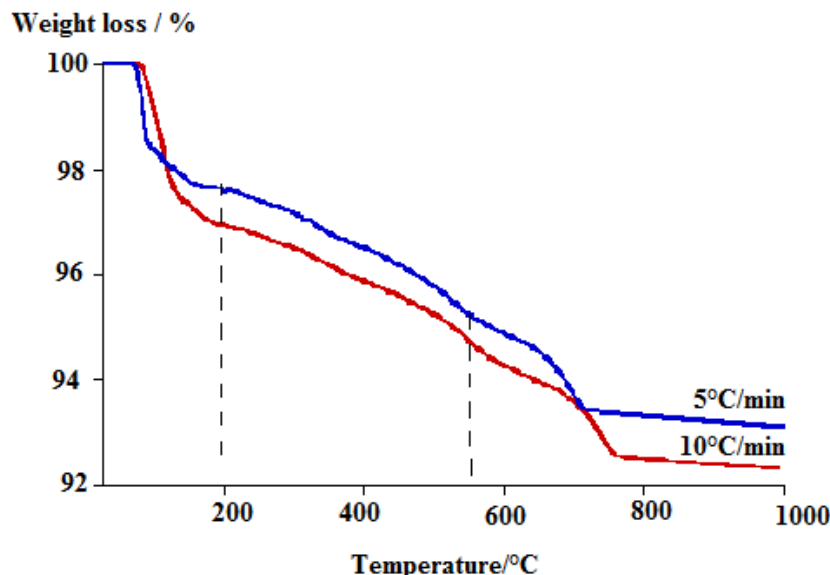


Figure 3. TG curves of the OST100 at two heating rates (5 and $10^{\circ}\text{C min}^{-1}$)

For completing study of the surface characteristic, the surface developed by unit mass of the solid, which takes into account all irregularities of surface at molecular scale, is one of the most important physico-chemical properties. The measure of the specific surface of the OST samples was realized by multi-points N_2 -sorption isotherms. In the case of OST100 and OST550, their isotherms correspond to mesoporous materials, opposite to that calcined OST950, which presents micropores. Further, the BET analysis shows that the surface area of dried OST100 ($27 \text{ m}^2 \text{ g}^{-1}$) is much higher than that of OST550 ($23 \text{ m}^2 \text{ g}^{-1}$) and OST950 ($3.5 \text{ m}^2 \text{ g}^{-1}$) related to the granular growth that reduced the surface pores. This is confirmed by calculation of the pore size distribution using the BJH model indicating a large distribution toward 3.7 nm for OST100 and OST550 that slightly narrows down to 20 nm for OST950.

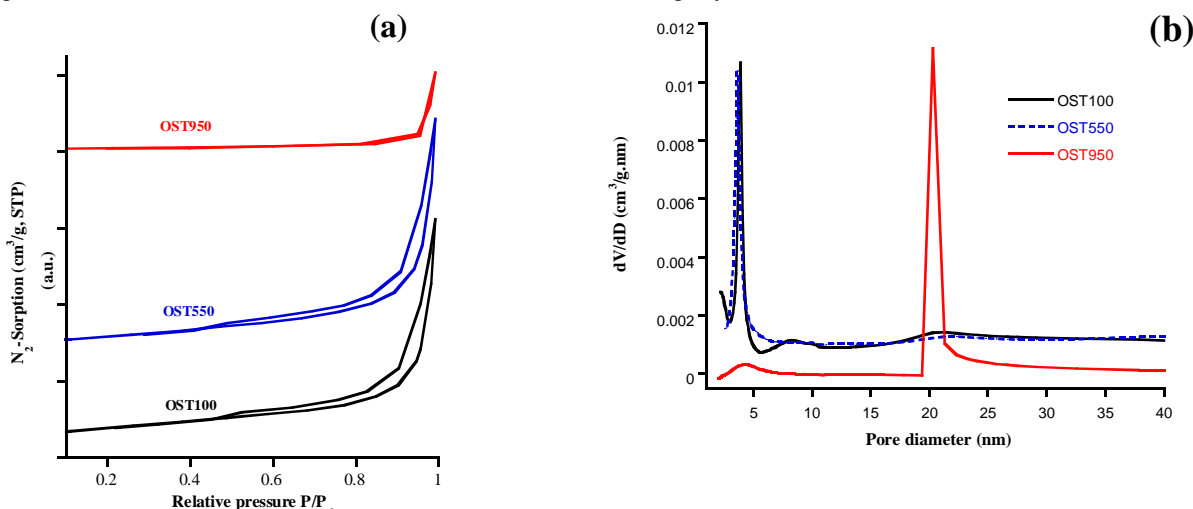


Figure 4: N_2 -sorption isotherms (a) and pore distribution from BJH calculation (b) for OST samples

Consequently, the pore distributions are mainly due to the texture of the silica in various environments among which the existence or the absence of the organic matter allocates in OST matrix.

3.2. Environmental application for antibiotic remediation

In a first step, the effect of contact time on the ciprofloxacin adsorption was studied for an initial concentration of 20 mg L⁻¹ and an adsorbent dose of 2 g L⁻¹ at room temperature and a initial pH=5.6 (Fig.5). First, CIP antibiotic appears the higher efficiently adsorbed specie for both OST100 and OST550 sorbents than that of OST950, with nearly delay required to reach equilibrium. Hence, the contact time upon the CIP removal by OST was determined to be 4 hours.

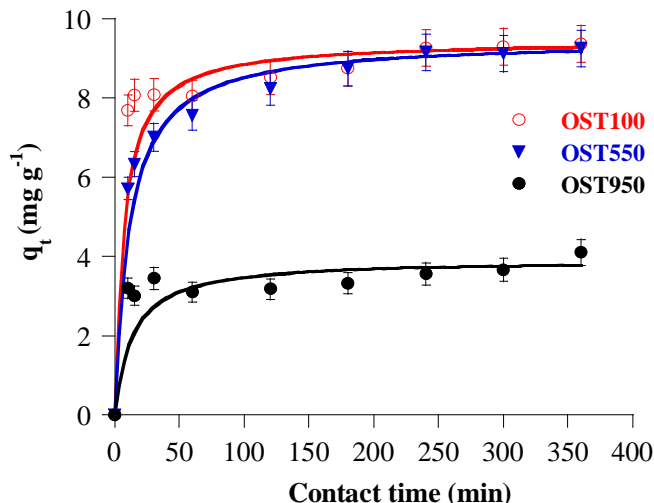


Figure 5: Evolution of the amount of sorbed ciprofloxacin (q_t) with contact time t on OST100, OST550 and OST950 adsorbents. Plain lines correspond to the curve obtained by fitting the data with the pseudo second order equation

For an initial concentration of 20 ppm of initial concentration of CIP antibiotic, the maximal adsorbed quantities on dried oil shale OST100 and calcined OST550 (9.30 mg.g⁻¹) are more important for that of calcined at 950°C (OST950) (3.66 mg.g⁻¹). Therefore, the removal of CIP by OST100 and OST550 is close to 93% and can be considered, as a new kind of adsorbent could be effective for the treatment of this antibiotic rich wastewater. However, the calcination of OST at 950°C degrades the CIP adsorption property. The fit of these data with Lagergren first order and pseudo-second order models were successfully attempted. Table 1 shows the adsorption kinetic parameters of pseudo-first-order and pseudo-second-order models. The correlation coefficient R^2 indicates that the second-order kinetic equation agrees better to the experimental data. It is more likely that the rate-limiting step is chemical adsorption and the adsorption behaviour may involve a complexation reaction with the cationic form of CIP whereas the protonated amine groups become prone to interact with oxide phases (SiO₂, Al₂O₃ and Fe₂O₃) containing OST mineral, in the addition to that of the contribution of carboxylate function with positively charge of OST surface [28]. For well-suited model, pseudo second order, the calculated equilibrium sorption capacities were 9.45, 9.46 and 3.93 mg g⁻¹ for OST100, OST550 and OST950 respectively, while the values of the rate constant, k_2 , were found 0.015, 0.009 and 0.002 min⁻¹, respectively, suggesting that the heat treatment of OST affects the kinetic of the ciprofloxacin removal from water. Therefore, the pseudo-first order model does not show a good compliance with experimental data, as shown in Table 1, where gives sorption capacities, $q_{e,1}$ significantly lower than experimental data with low R^2 values.

Table 1. Kinetic rate constants (k) and adsorption capacities (q_e) as obtained for different models for CIP antibiotic sorption by OST100, OST550 and OST950 adsorbents. R^2 indicate the correlation coefficients for the linear fits

Kinetic model	Pseudo first order			Pseudo second order		
	k_1 (min ⁻¹)	$q_{e,1}$ (mg g ⁻¹)	R^2	k_2 (min ⁻¹)	$q_{e,2}$ (g mg ⁻¹ .min ⁻¹)	R^2
OST100	0.0123	2.92	0.9167	0.015	9.45	0.9993
OST550	0.0122	3.64	0.9958	0.009	9.46	0.9995
OST950	0.0030	1.28	0.9732	0.002	3.93	0.9928

Based on previous kinetics data, sorption isotherms were obtained after 4 hours as contact time, showing that OST100 exhibits a higher ciprofloxacin adsorption capacity than OST550 and OST950. The isotherms of adsorption were realized with various initial concentrations of CIP pollutant (Fig.6).

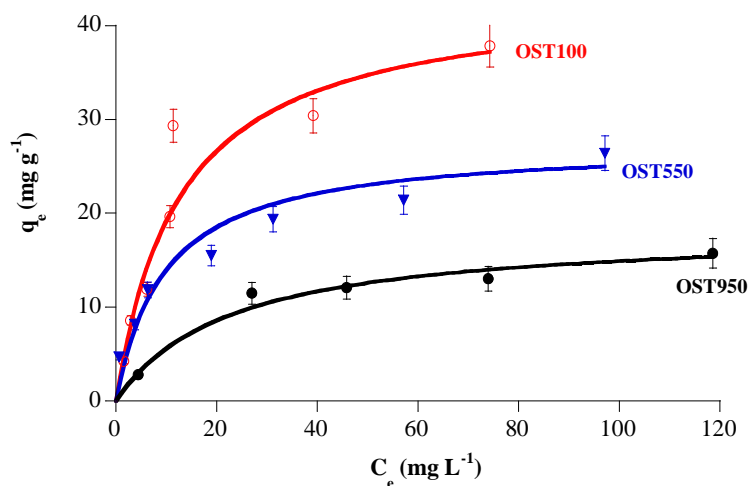


Figure 6: Variation of sorbed antibiotic content (q_e) with antibiotic equilibrium concentration onto OST adsorbents. Plain lines correspond to the curve obtained by fitting the data with the Langmuir equation

Experimental data are fitted using the Langmuir and Freundlich models where their corresponding parameters are summarized in Table 2. We note that the Langmuir equation is the most fitting model and the maximal capacities are near to experimental values. When the Freundlich model was applied, low correlation coefficients, R^2 , were obtained. The fixed quantity of the CIP by the OST shale is more important or sometime comparable than those cited in the literature [29-31]. This related to impact of the nature of chemical elements onto OST surface. As we already signaled him in our various works, the adsorption process depends on surface composition, specific surface and therefore of the number of the active sites into adsorbent surface [32-33].

Table 2 Langmuir and Freundlich constants for CIP antibiotic sorption on the OST100, OST550 and OST950 adsorbents

	$q_{\text{max,exp}}$	Langmuir			Freundlich		
		$q_{e,\text{max}}$	β	R^2	$\log K_f$	$1/n$	R^2
OST100	37.7	43.4	0.034	0.9853	0.666	0.544	0.9353
OST550	24.9	27.4	0.048	0.9944	0.755	0.338	0.9244
OST950	15.3	18.2	1.02	0.9413	0.053	0.581	0.9413

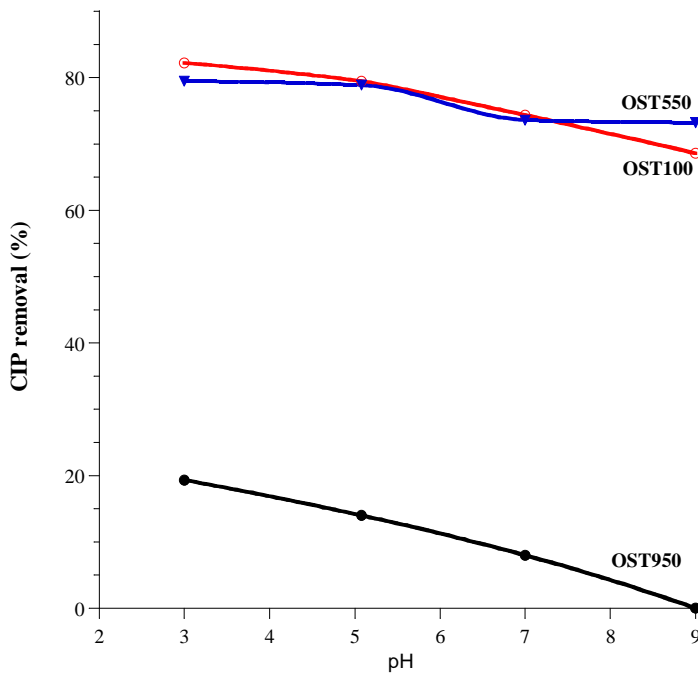


Figure 7: Effect of the pH of the solution on the removal of CIP antibiotic by OST adsorbents

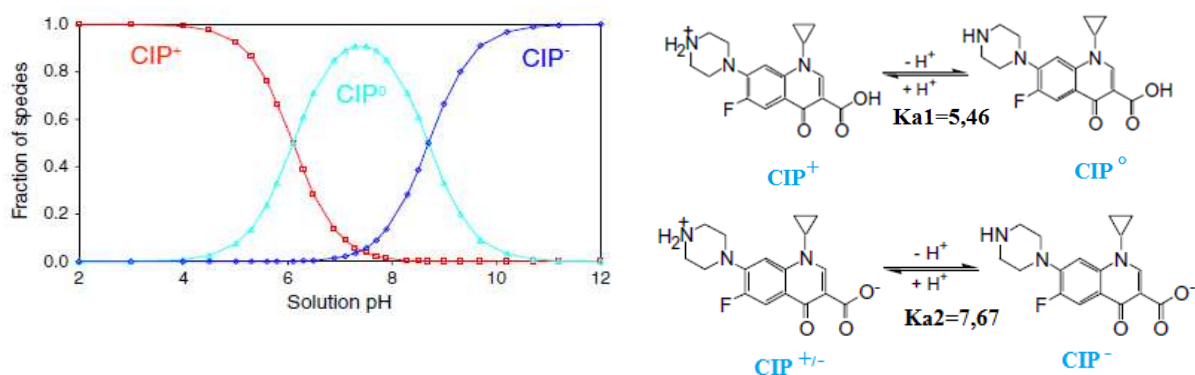


Figure 8: pH-dependent ciprofloxacin in the solution [34]

The pH value of the solution has a significant impact on the removal of CIP antibiotic, because it determines the surface charge of OST adsorbent and the degree of ionization and speciation of adsorbate. Figure 7 illustrates the effect of pH value on the adsorption of CIP antibiotic onto OST surface. The most removal capacity is obtained at acid pH and then decreased with alkaline pH. In the solution, ciprofloxacin antibiotic exists in different forms According to its pK_a (Fig. 8). The higher CIP removal was achieved when the solution pH was less than the pK_{a2} value of CIP, above which adsorption coefficient decreased significantly. In fact, the both cationic and zwitterion forms of CIP could adsorb better on OST shale, where the positively charged amino was able to contribute to the CIP removal. When the pH solution was greater than pK_2 , an anion played a dominant role in CIP speciation (CIP^-) and a significant repulsion was induced between the negatively charged shale surface and CIP^- anion, which its removal was significantly reduced. The similar pH profile was observed for the CIP adsorption on OST100 and OST550. Hence, the acid medium was shown to be the most optimal for the removal of CIP antibiotic from wastewater.

The adsorbent dose in the solution can affect the capacity of CIP sorption to show the optimum dose of ciprofloxacin antibiotic (Fig.9). The removal of ciprofloxacin (in %) from solution progressively increases with adsorbent dose except for OST950 case. From the figure, it was observed that the percentage removal of the ciprofloxacin increases with increasing the adsorbent dose until 2 g L^{-1} and further increase of the adsorbent dose did not provide more increment in the percentage of the CIP removed. Therefore, 2 g L^{-1} dose of the OST adsorbent was used in all our studies. Non-significant increase observed when the adsorbent doses were increased up 2 g L^{-1} , suggesting that after a certain dose of adsorbent, the maximum adsorption is attained and the amount of the complexed CIP with OST surface.

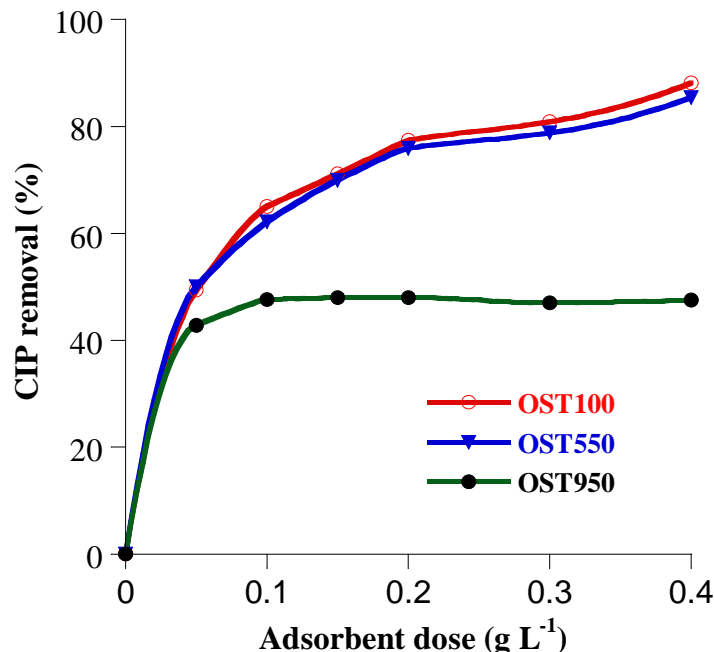


Figure 9: Optimal adsorbent concentrations for the adsorption of CIP by OST shale

To evaluate the regeneration of the OST550 shale, three consecutive adsorption-desorption cycles were conducted with 20 mg·L⁻¹ of CIP solution. A first sorption was performed and then the powder was treated to 550°C. The regeneration efficiency reached 89 %, 80% and 78% for ciprofloxacin at the first, second and third cycle, respectively. Therefore, in terms of adsorbent performance, the loss of sorption capacity observed after thermal treatment is related to the major degradation of CIP antibiotic at 550°C and the structure stability of OST adsorbent. As a result, adsorption/desorption experiments also indicate that OST550 adsorbent represents an interesting compromise for the CIP removal and its recyclability at 550°C for the degradation of major CIP part.

CONCLUSION

In this study, structural and textural properties of oil shale from Tanger (Morocco) are presented. The examination of this shale, the XRD results indicate the presence of the main inorganic component quartz-SiO₂ with oxide phases. The thermal analysis has shown that small quantity of the organic component is actually still present (8 wt.%) compared to other Moroccan oil shales.

The adsorption isotherms and kinetics data obtained for the removal of ciprofloxacin antibiotic from aqueous solution would be perfectly using dried and calcined oil shale at 550°C. The adsorption is affected by the initial concentration of antibiotic, adsorbent dose and pH of the solution. The produced material OST550 is not expensive, easily produced, and recyclable and solve the environmental issue.

REFERENCES

- [1] A. Ghauch, A. Tuqan, H.A Assi, *Environ. Pollut.* **2009**, 157, 1626–1635
- [2] J. Gao, JA. Pedersen, *Environ. Sci. Technol.* **2005**, 39, 9509-9516.
- [3] G. Moulin, P.Cavalie, I. Pellanne, A. Chevance, A. Laval, Y. Millemann, P. Colin, C. Chauvin. *J. Antimicrob. Chemother.* **2008**, 62, 617-625.
- [4] K. Kummerer, *Chemosphere* **2009**, 75, 435–441.
- [5] K. Kumar, S.C. Gupta, Y. Chander, A.K Singh, *Adv. Agron.* **2005**, 87, 1–54.
- [6] Y.C. Lin, T.H. Yu, C.F. Lin, *Chemosphere* **2008**, 74, 131-141.
- [7] K. Kümmeler, *Chemosphere* **2009**, 75, 417-434.
- [8] S. Thiele-Bruhn, *J. Plant Nutr. Soil Sci.* **2003**, 166, 145-67.
- [9] M.S.Díaz-Cruz, M.J. López de Alda, D.Barceló, *Trends Anal. Chem.* **2003**, 22, 340-348.
- [10] F.Hernández, A. Rivera, A. Ojeda, T. Zayas, L. Cedillo, *J. Environ. Sci. Engin. A* **2012**, 1, 448-453.
- [11] C.Gu , K.G. Karthikeyan, *Environ. Sci. Technol.* **2005**, 39, 9166–9173.
- [12] S. Ichcho, E. Khouya, S. Fakhi, M. Ezzine, H. Hannache, R. Pallier, R. Naslain, *Journal of Hazardous Materials* **2005**, 118, 45-51.
- [13] S. Saoiabi, S. El Asri, A. Laghzizil, T. Coradin, K. Lahllil, *Materials letters*, **2010**, 64 2679-2681.
- [14] V. Bruan, M. Halim, M. Ziyad, C. Largeau, A. Amblès, *Journal of Analytical and Applied Pyrolysis*, **2001**, 61, 165-179.
- [15] N. Regina Camargo Fernandes Machado, Denise Maria Malachini Miotto, *Fuel* **2005**, 84 2289–2294.
- [16] S. Zhu, P.R.F. Bell, P.F. Greenfield, *Water Research* **1988**, 22, 1331-1337
- [17] Z. Al-Qodaha, A.T. Shawaqfehb, W.K. Lafia, *Desalination* **2007**, 208, 294–301.
- [18] Z Al-Qodah, *Water Research* **2000**, 34, 4295-4303
- [19] E. Tütem, R. Apak, Ç. F. Üna, *Water Research* **1998**, 32, 2315-2324.
- [20] S. Ortaboy, G. Atun, *Annals of Nuclear Energy* **2014**, 73, 345-354
- [21] R. Shawabkeh, A. Al-Harahsheh, A. Al-Otoom, *Sep. Purif. Technol.* **2004**, 40, 251-257.
- [22] S. Babel, T.A. Kurniawan, *J. Hazard. Mater.B* **2003**, 97, 219-243.
- [23] V. Srihari, V., A. Das, A., *Desalination* **2008**, 225, 220-234.
- [24] Y.S.Ho, *J. Hazard Mater.* **2006**, 136, 681-689.
- [25] A. Aboulkas, K El Harti, *Journal of Fuel Chemistry and Technology* **2009**, 37, 659-667
- [26] M. ELHarti, K. Legrouri, E. Khouya, H. Hannache, S. Fakhi, M. EL Boucchi, N. Hanafi, A. Solhy, B. Hammouti, *Der Pharma Chemica* **2012**, 4, 2130-2139.
- [27] A.K. Abourriche, M. Oumam, H. Hannache, M. Birot, Y. Abouliatim, A. Benhammou, Y. El Hafiane, A.M. Abourriche, R. Pailler, R. Naslai, *The Journal of Supercritical Fluids* **2013**, 84, 98-104.
- [28] S. Rakshit, D. Sarkar, E. J. Elzinga, P. Punamiya, R. Datta, *Journal of Hazardous Materials* **2013**, 246-247, 221-226
- [29] El-Said Ibrahim El-Shafey , Haider Al-Lawati, Asmaa Soliman Al-Sumri, *Journal of Environmental Sciences* **2012**, 24, 1579–1586
- [30] Z. Liu, P. Sun, S.G. Pavlostathis, X. Zhou, Y. Zhan, *Bioresource Technology* **2013**, 144, 644-651

-
- [31] S.Wu, X. Zhao, Y. Li, C. Zhao, Q. Du, J. Sun, Y. Wang, X. Peng, Y.i Xia, Z.Wang, L. Xia, *Chemical Engineering Journal* **2013**, 230, 389-395.
 - [32] S. El Asri, A. Laghzizil, T. Coradin, A. Saoiabi, A. Alaoui, R. M'hamed, *Colloids and Surfaces A*, **2010**, 362, 33-38.
 - [33] S. Saoiabi, S. El Asri, A. Laghzizil, A. Saoiabi, J.L. Ackerman, T. Coradin, *Chemical Engineering Journal* **2012**, 211–212, 233-239.
 - [34] D.Vasudevan, G.L. Bruland, B.S.Torrance, V.G. Upchurch, A.A.MacKay, *Geoderma* **2009**, 151, 68-76.